Inorg. Chem. **2003**, *42*, 3595–3601

Enhancing the Stability of Trinickel Molecular Wires and Switches: Ni_3^{6+}/Ni_3^{7+}

John F. Berry,[†] F. Albert Cotton,*[,†] Tongbu Lu,[†,‡] Carlos A. Murillo,*[,†] and Xiaoping Wang[†]

Laboratory for Molecular Structure and Bonding, Department of Chemistry, P.O. Box 30012, Texas A&M University, College Station, Texas 77842-3012, and School of Chemistry & Chemical Engineering, Sun Yat-Sen University, Guangzhou 510275, P. R. China

Received February 12, 2003

This paper describes in detail four new compounds that contain extended metal atom chains (EMACs) of three nickel atoms wrapped by either di(2-pyridyl)amide (dpa) or the new homologous ligand with an ethyl group at the para position of each pyridyl group, depa, and compares them to the precursor $Ni_3(dpa)_4Cl_2$ (**1**) and the oxidized and rather unstable $Ni_3(dpa)_4(PF_6)_3$ (**2**). The new molecules are $Ni_3(depa)_4Cl_2$ (**3**), $Ni_3(depa)_4(PF_6)_3$ (**4**), $[Ni_3(dpa)_4(CH_3CN)_2](PF_6)_2$ (**5**), and $[Ni_3(depa)_4(CH_3CN)_2](PF_6)_2$ (**6**). These compounds are fully described as to preparation, elemental composition, structure, infrared spectra, ^1H NMR spectra (where possible), electrochemistry, magnetic susceptibility, and an EPR spectrum for **4**. The effects of (a) introducing the ethyl substituents on the ligands, (b) replacing axial anions by neutral axial ligands, and (c) oxidizing the Ni_3 chains are reported and discussed. The point of major interest is how oxidation profoundly alters the electronic structure of the EMAC.

1. Introduction

We have recently reported[1] on the effects of introducing ethyl substituents into the pentanickel compound $Ni_5(tpda)_4Cl_2$, where tpda is the dianion **a**, to obtain $Ni_5(etpda)_4Cl_2$, where etpda is **b**. We have now completed a similar but more extensive study of analogous trinickel compounds. While it might seem more logical to publish the work on the trinickel compounds first, the actual course of research did not allow us to do that.

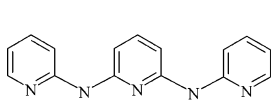

a

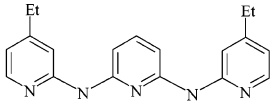

b

The entire field of extended metal atom chains (EMACs) can be traced back to 1968 when purple $Ni_3(dpa)_4Cl_2$, **1** (dpa = anion of di(2-pyridyl)amine (shown as **c**)), was reported but not correctly formulated.[2] With the structure correctly determined in 1991,[3] the field can truly be said to have begun, and in the ensuing years an immense growth has occurred, primarily in this laboratory[4] and that of Prof. S.-M. Peng in Taipei.[5]

Quite apart from the historical importance of **1**, it and its derivatives and homologues continue to be of prime importance in a fundamental understanding of the entire class of EMACs. For this reason we have continued to investigate very actively **1** and its relatives that also contain nickel. In 1999 we published a definitive study of $Ni_3(dpa)_4Cl_2$ itself.[6] We have now proceeded well beyond **1** itself to determine the influence of three factors: (1) oxidation to produce $Ni_3(dpa)_4(PF_6)_3$,[7] **2**; (2) change of axial ligands; and (3) the effect of substituents on the dpa ligand on the characteristics of the Ni_3 chain. In our report of the oxidation of **1** to produce

* To whom correspondence should be addressed: cotton@tamu.edu (F.A.C.); murillo@tamu.edu (C.A.M.).
† Texas A&M University.
‡ Sun Yat-Sen University.

(1) Berry, J. F.; Cotton, F. A.; Lei, P.; Lu, T.; Murillo, C. A. *Inorg. Chem.*, in press.
(2) Hurley, T. J.; Robinson, M. A. *Inorg. Chem.* **1968**, *7*, 33.
(3) Aduldecha, S.; Hathaway, B. *J. Chem. Soc., Dalton Trans.* **1991**, 993.
(4) See for example: (a) Cotton, F. A.; Daniels, L. M.; Murillo, C. A.; Pascual, I. *J. Am. Chem. Soc.* **1997**, *119*, 10223. (b) Clérac, R.; Cotton, F. A.; Daniels, L. M.; Dunbar, K. R.; Kirschbaum, K.; Murillo, C. A.; Pinkerton, A. A.; Schultz, A. J.; Wang, X. *J. Am. Chem. Soc.* **2000**, *122*, 6226. (c) Cotton, F. A.; Daniels, L. M.; Lu, T.; Murillo, C. A.; Wang, X. *J. Chem. Soc., Dalton Trans.* **1999**, 517.
(5) See for example: (a) Yang, E.-C.; Cheng, M.-C.; Tsai, M.-S.; Peng, S.-M. *J. Chem. Soc., Chem. Commun.* **1994**, 2377. (b) Sheu, J.-T.; Lin, C.-C.; Chao, I.; Wang, C.-C.; Peng, S.-M. *Chem. Commun.* **1996**, 315. (c) Zhu, L.-G.; Peng, S. M. *Wuji Huaxue Xuebao* **2002**, *18*, 117.
(6) Clérac, R.; Cotton, F. A.; Dunbar, K. R.; Murillo, C. A.; Pascual, I.; Wang, X. *Inorg. Chem.* **1999**, *38*, 2655.
(7) (a) Berry, J. F.; Cotton, F. A.; Daniels, L. M.; Murillo, C. A. *J. Am. Chem. Soc.* **2002**, *124*, 3212. (b) Berry, J. F.; Cotton, F. A.; Daniels, L. M.; Murillo, C. A.; Wang, X. *Inorg. Chem.*, **2003**, *42*, 2418.

10.1021/ic0341486 CCC: $25.00
Published on Web 05/02/2003

2 we discussed how, upon oxidation, the Ni−Ni separations of about 2.43 Å decrease to 2.28 Å. Such a diminution by 0.15 Å is contrary to what would be expected for an increase by one positive charge on proximate but nonbonded, positively charged Ni ions. Thus it was concluded that metal−metal bond formation is responsible for the large contraction in Ni−Ni separations. It can be envisioned that a molecular switch[8] could be produced as a consequence of a change from a non-interacting (presumably nonconducting) chain of metal atoms to an interacting (presumably conducting) chain by an appropriate change in the applied potential. We have now studied some of the factors that affect the stability of these trinickel species, especially the oxidized ones, and we have produced a considerably more thermally stable switch. The importance of having products that are easily handled at room temperature (and above) cannot be overestimated. A full report on that work, which deals with four new compounds, is presented here. The new compounds are (**3**) $Ni_3(depa)_4Cl_2$, (**4**) $Ni_3(depa)_4(PF_6)_3$, (**5**) $[Ni_3(dpa)_4(CH_3CN)_2](PF_6)_2$, and (**6**) $[Ni_3(depa)_4(CH_3CN)_2](PF_6)_2$ where depa is the anion of 4,4′-diethyl-2,2′-dipyridylamine, the diethyl-substituted ligand, **d**.

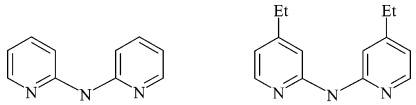

c **d**

2. Experimental Section

Unless otherwise stated, reactions were carried out under nitrogen with the use of standard Schlenk techniques. Anhydrous $NiCl_2$ and $AgPF_6$ were purchased from Strem Chemicals, and 4-ethylpyridine was purchased from Aldrich. All the solvents used were dried and distilled under N_2 by following standard procedures. $Ni_3(dpa)_4Cl_2$ was prepared according to our previous report,[7b] and 2-amino-4-ethylpyridine was prepared according to a published method.[9]

Physical Measurements. Elemental analyses were performed by Canadian Microanalytical Services in British Columbia, Canada. The IR spectra were recorded on a Perkin-Elmer 16PC FT-IR spectrophotometer using KBr pellets. ^{1}H NMR spectra were obtained on a VXR-300 NMR spectrometer. Cyclic voltammograms (CVs) were taken on a BAS 100 electrochemical analyzer with $Bu^n_4NPF_6$ (0.1 M) electrolyte, Pt working and auxiliary electrodes, a Ag/AgCl reference electrode, and a scan rate of 100 mV/s. The magnetic susceptibility data were collected on a Quantum Design SQUID magnetometer MPMS-XL from 2 to 300 K at a field of 1000 G on finely ground, vacuum-dried samples. The data were corrected for the sample holder and for the diamagnetic contributions calculated from Pascal's constants. The X-band EPR spectrum of a THF glass of **4** was recorded at 6 K on a Bruker ESP 300 spectrometer.

2,2′-Di(4-ethyl)pyridylamine (Hdepa). This was made by a modification of a literature reaction for a related compound.[10] A mixture of 2-amino-4-ethylpyridine (10.0 g, 81.0 mmol) and 2-amino-4-ethylpyridine hydrochloride (12.9 g, 81.0 mmol) was heated at 290 °C under a nitrogen atmosphere for 8 h. After cooling to room temperature, 40 mL of water was added; the resulting solution was made basic by addition of solid NaOH and extracted with chloroform (3 × 50 mL). After the chloroform extracts were dried over K_2CO_3, the chloroform was evaporated, and the residue was distilled under vacuum (0.2 mm). This gave two fractions. The first contained about 2 g of unreacted 2-amino-4-ethylpyridine. The second fraction contained the product, which was distilled at 135−140 °C as a yellow oil (7.0 g, 38%). After standing overnight, the oil became a light yellow solid, which was purified by sublimation. ^{1}H NMR ($CDCl_3$, 300 MHz, δ): 8.12 (d, J = 4.8 Hz, 2H), 7.82 (br s, 1H), 7.36 (s, 2H), 6.68−6.66 (dd, 2H), 2.66−2.58 (q, J = 7.8 Hz, 4H), 1.22 (t, J = 7.2 Hz, 6H).

$Ni_3(depa)_4Cl_2$, 3. A 100 mL round-bottom flask was charged with anhydrous $NiCl_2$ (0.26 g, 2.0 mmol), Hdepa (0.45 g, 2.0 mmol), and naphthalene (10 g). The mixture was heated at 185−190 °C for 5 min, and then *n*-butanol (3 mL) was carefully added; heating was continued while the system was purged with nitrogen until the *n*-butanol completely evaporated. Then, a solution of *t*-BuOK (0.23 g, 2.0 mmol) in 5 mL of *n*-butanol was added dropwise. Heating was continued until the remaining *n*-butanol was evaporated completely. After the mixture was cooled to about 80 °C, hexanes (3 × 60 mL) were used to remove naphthalene. The remaining deep purple solid was extracted with toluene (2 × 10 mL) and this solution was then layered with hexanes. After 1 week, a large crop of deep purple crystals of **3**·$0.5C_6H_{14}$ formed. Yield: 0.38 g, 66%. Anal. Calcd for $C_{59}Cl_2H_{71}N_{12}Ni_3$ ($Ni_3(depa)_4Cl_2$·$0.5C_6H_{14}$): C, 59.29; H, 5.99; N, 14.06. Found: C, 59.37; H, 5.98; N, 13.91. IR (KBr, cm^{-1}): 3448 (br, w), 3056 (w), 2965 (s), 2928 (m), 2869 (m), 1608 (s), 1536 (s), 1473 (s), 1414 (s), 1346 (s), 1290 (s), 1227 (m), 1179 (s), 1126 (w), 1061 (m), 1014 (s), 937 (s), 813 (s), 739 (m), 656 (w), 544 (m), 444 (s).

$Ni_3(depa)_4(PF_6)_3$, 4. A Schlenk flask containing $Ni_3(depa)_4Cl_2$ (0.120 g, 0.104 mmol) and $AgPF_6$ (0.105 g, 0.416 mmol) was charged with 15 mL of CH_2Cl_2 at −78 °C. The resulting solution was stirred at −78 °C in the dark for 1 h to give a deep blue mixture, which was filtered while cold through Celite to remove AgCl and Ag. The filtrate was layered with hexanes and kept in a freezer. After about 1 week, large blue crystals of **4**·$3CH_2Cl_2$ formed. Yield: 0.14 g, 76%. Anal. Calcd for $C_{57.5}Cl_3F_{18}H_{67}N_{12}Ni_3P_3$ ($Ni_3(depa)_4(PF_6)_3$·$1.5CH_2Cl_2$): C, 42.02; H, 4.11; N, 10.23. Found: C, 41.98; H, 4.24; N, 10.45. IR (KBr, cm^{-1}): 3435 (br, m), 2970 (w), 1616 (s), 1535 (w), 1476 (m), 1426 (vs), 1230 (w), 1181 (w), 1093 (br, m), 843 (vs), 734 (w), 558 (m), 472 (w).

$[Ni_3(dpa)_4(MeCN)_2](PF_6)_2$, 5. A dark purple solution of $Ni_3(dpa)_4Cl_2$ (317 mg, 0.342 mmol) in 15 mL of acetonitrile was stirred as a solution of $AgPF_6$ (173 mg, 0.684 mmol) in 15 mL of acetonitrile was added dropwise. The mixture became more intensely purple, and a white precipitate was observed. After stirring for several hours, the mixture was filtered with the aid of Celite to give a clear, dark purple solution. This solution was concentrated by means of vacuum and layered with diethyl ether. Within 1 week, large block-shaped purple crystals of **5**·3.90 MeCN grew along the sides of the flask. Yield: 0.325 g, 77%. IR, (KBr, cm^{-1}): 3448 (w, br), 3026 (w), 2965 (w), 2500 (vw), 2291 (w, CN), 1604 (s), 1595 (s), 1550 (m), 1469 (vs), 1460 (vs), 1425 (vs), 1358 (s), 1315 (m), 1283 (m), 1263 (w), 1243 (w), 1150 (m), 1111 (m), 1053 (w), 1017 (m), 894 (w), 839 (vs), 763 (s), 740 (m), 641 (w), 557 (m), 517 (w), 497 (w), 426 (m). Anal. Calcd for $C_{40}H_{34}N_{12}OP_2F_{12}Ni_3$: C, 41.25; H, 2.94; N, 14.43. Found: C, 41.54; H, 3.41; N, 14.88.

$Ni_3(depa)_4(CH_3CN)_2(PF_6)_2$, 6. A Schlenk flask containing $Ni_3(depa)_4Cl_2$ (0.20 g, 0.17 mmol) and $AgPF_6$ (0.090 g, 0.36 mmol)

(8) For a recent review on molecular electronics, see: Carroll, R. L.; Gorman, C. B. *Angew. Chem., Int. Ed.* **2002**, *41*, 4378.
(9) Hansch, C.; Carpenter, W.; Todd, J. *J. Org. Chem.* **1958**, *23*, 1924.
(10) (a) Baxter, C. E.; Rodig, O. R.; Schlatzer, R. K.; Sinn, E. *Inorg. Chem.* **1979**, *18*, 1918. (b) Dyadyusha, G. G.; Verbovskaya, T. M.; Kiprianov, A. I. *Ukr. Khim. Zh. (Russ. Ed.)* **1966**, *32*, 357.

Table 1. Crystal Data

	3·0.5hexane	**4**·3CH_2Cl_2	**5**·3.14CH_3CN	**6**·0.33H_2O
formula	$C_{59}H_{71}Cl_2N_{12}Ni_3$	$C_{59}H_{70}Cl_6F_{18}N_{12}Ni_3P_3$	$C_{50.27}H_{47.41}F_{12}N_{17.14}Ni_3P_2$	$C_{60}H_{70.67}F_{12}N_{14}Ni_3O_{0.33}P_2$
fw	1195.31	1771.01	1357.70	1459.38
cryst syst	tetragonal	monoclinic	triclinic	cubic
space group	$P\bar{4}n2$	$P2_1/n$	$P\bar{1}$	$Pn\bar{3}n$
a, Å	19.0825(7)	13.920(1)	12.56(1)	21.5984(5)
b, Å	19.0825(7)	31.703(3)	12.802(9)	21.5984(5)
c, Å	15.771(1)	16.727(1)	20.01(2)	21.5984(5)
α, deg	90	90	107.26(2)	90
β, deg	90	95.023(2)	98.83(3)	90
γ, deg	90	90	101.54(5)	90
V, Å^3	5743.0(5)	7353(1)	2932(4)	10075.5(4)
Z	4	4	2	6
d(calc), g cm^{-3}	1.382	1.600	1.538	1.443
R1,[a] wR2[b] [$I > 2\sigma(I)$]	0.0323, 0.0888	0.0756, 0.1757	0.0908, 0.2365	0.0508, 0.1319
R1,[a] wR2[b] (all data)	0.0383, 0.0955	0.0993, 0.1884	0.1185, 0.2653	0.0729, 0.1639

[a] $R1 = \sum||F_o| - |F_c||/\sum|F_o|$. [b] $wR2 = [\sum[w(F_o^2 - F_c^2)^2]/\sum[w(F_o^2)^2]]^{1/2}$, $w = 1/\sigma^2(F_o^2) + (aP)^2 + bP$, where $P = [\max(0 \text{ or } F_o^2) + 2(F_c^2)]/3$.

was charged with 15 mL of acetonitrile. The resulting solution was stirred at room temperature in the dark for 3 h to give a deep purple mixture, which was filtered through Celite to remove AgCl. To the filtrate was added 15 mL of ether. The clear solution was allowed to evaporate slowly in air. After about 2 weeks, deep purple crystals of **6**·0.33H_2O formed from the solution. Yield: 0.12 g, 48%. IR (KBr, cm^{-1}): 3427 (s, br), 2969 (s), 2368 (w), 2281 (w, CN), 1612 (vs), 1535 (s), 1474 (s), 1417 (vs), 1345 (m), 1229 (w), 1181 (m), 1060 (w), 1016 (w), 938 (w), 844 (vs), 738 (w), 557 (m), 447 (m).

Crystallography. In each case, a suitable crystal was mounted on the end of a quartz fiber with a small amount of stopcock grease and was transferred to a goniometer head. X-ray diffraction data for **3**·0.5C_6H_{14}, **4**·3CH_2Cl_2, and **6**·0.33H_2O were collected on a Bruker Smart 1000 CCD area detector system at 213 K. Data were corrected for Lorentz and polarization effects using the program SAINTPLUS.[11] Absorption corrections were applied using SADABS.[12] These three structures were solved by direct methods.

For **5**·3.14MeCN X-ray data were gathered on a Nonius FAST diffractometer at 213 K using the software program MADNES.[13] Reflections for indexing were found via a routine which collects a series of images from several different sections of reciprocal space. The reflections showed signs of high mosaicity by the broadening in ω. A triclinic unit cell was refined using 247 strong reflections with $18.1° < 2\theta < 41.8°$. The cell dimensions were confirmed by examination of axial images. The program PROCOR[14] was used to process the integrated data into SHELX format. The data were corrected for Lorentz and polarization effects, and absorption corrections were applied using the program SORTAV.[15] The structure was solved using the Patterson method.

In all structures, hydrogen atoms were placed at calculated positions based on a riding model. Some of the ethyl groups in **3**·0.5C_6H_{14}, **4**·3CH_2Cl_2, and **6**·0.33H_2O, hexane and dichloromethane in **3**·0.5C_6H_{14} and **4**·3CH_2Cl_2, and PF_6 anions in **5**·3.90MeCN and **6**·0.33H_2O were found to be disordered. All refinement cycles were performed using the SHELXL-97 program.[16] The crystallographic data are listed in Table 1.

3. Results and Discussion

Preparative Chemistry. The precursor of ligand **d**, Hdepa, was prepared in moderate yield from commercially available starting materials. $Ni_3(depa)_4Cl_2$ (**3**) was prepared according to eq 1 using naphthalene as solvent, which allows the reaction temperature to be raised to 185−190 °C. Conversion of **3** to $Ni_3(depa)_4(PF_6)_3$ (**4**) was accomplished by reaction with an excess of $AgPF_6$ at −78 °C as shown in eq 2. By treating **3** with exactly 2 equiv of $AgPF_6$ in acetonitrile at 20−25 °C $[Ni_3(depa)_4(CH_3CN)_2](PF_6)_2$ (**6**) was obtained as shown in eq 3. The dpa analogue of **6**, namely, $[Ni_3(dpa)_4(CH_3CN)_2](PF_6)_2$ (**5**), was obtained in an analogous way from $Ni_3(dpa)_4Cl_2$ (**1**). Reaction 3 succeeds, in part, because $AgPF_6$ is a much milder oxidant in acetonitrile than it is in CH_2Cl_2.[17] This is no doubt attributable to the ability of CH_3CN to stabilize the Ag^+ ion.

$$3NiCl_2 + 4Hdepa + 4\ t\text{-BuOK} \xrightarrow{\text{BuOH, } C_{10}H_8} Ni_3(depa)_4Cl_2 + 4\ t\text{-BuOH} + 4KCl \quad (1)$$

$$Ni_3(depa)_4Cl_2 + 3AgPF_6 \xrightarrow{CH_2Cl_2} Ni_3(depa)_4(PF_6)_3 + Ag + 2AgCl \quad (2)$$

$$Ni_3(depa)_4Cl_2 + 2AgPF_6 + 2CH_3CN \xrightarrow{CH_3CN} [Ni_3(depa)_4(CH_3CN)_2](PF_6)_2 + 2AgCl \quad (3)$$

Structural Results. Crystal structures of **3**−**6** were solved and refined satisfactorily. Thermal ellipsoid drawings of the structures are shown in Figures 1−4, and some important dimensions are listed for compounds **1**−**6** in Table 2. More detailed comparison of these structures will be made below,

(11) *SAINTPLUS, V 6.28A Software for the CCD Detector System*; Bruker Analytical X-ray System, Inc.: Madison, WI, 2001.
(12) SADABS. Program for absorption correction using SMART CCD data based on the method of Blessing: Blessing, R. H. *Acta Crystallogr.* **1995**, *A51*, 33.
(13) Pflugrath, J.; Messerschmidt, A. MADNES, Munich Area Detector (New EEC) System, Version EEC 11/1/89, with enhancements by Enraf-Nonius Corp., Delft, The Netherlands. A description of MADNES appears in the following: Messerschmitt, A.; Pflugrath, J. *J. Appl. Crystallogr.* **1987**, *20*, 306.
(14) (a) Kabsch, W. *J. Appl. Crystallogr.* **1988**, *21*, 67. (b) Kabsch, W. *J. Appl. Crystallogr.* **1988**, *21*, 916.
(15) Program for absorption correction for Enraf-Nonius FAST diffractometer using the method of Blessing: Blessing, R. H. *Acta Crystallogr.* **1995**, *A51*, 33.
(16) Sheldrick, G. M. *SHELXTL97*; University of Göttingen: Göttingen, Germany, 1997.
(17) Connelly, N. G.; Geiger, W. E. *Chem. Rev.* **1996**, *96*, 877.

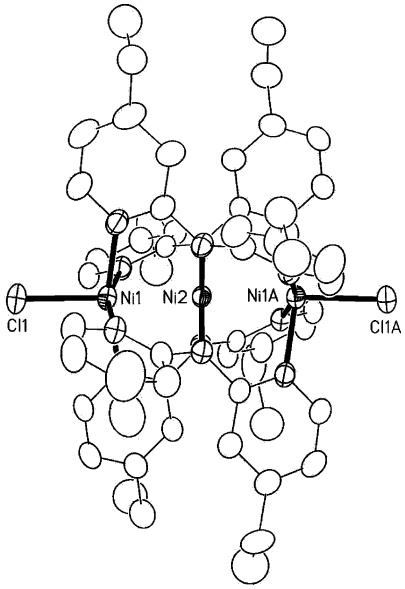

Figure 1. Thermal ellipsoid plot of **3** with ellipsoids drawn at the 50% probability level. Only one orientation of the disordered ethyl groups is shown; hydrogen atoms and solvent molecules have been omitted for clarity.

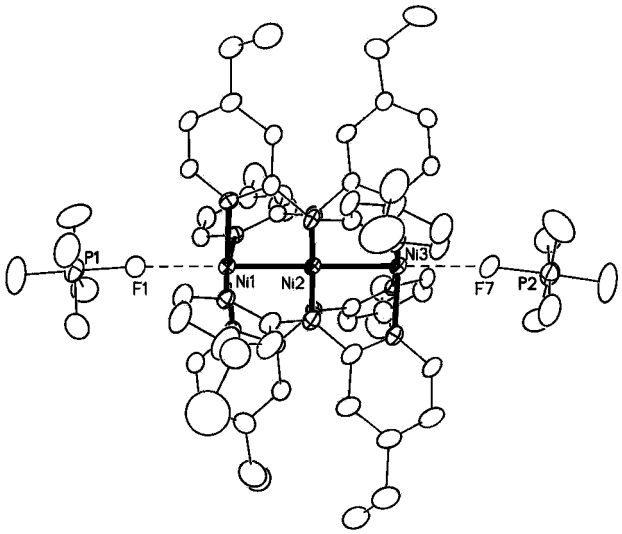

Figure 2. Thermal ellipsoid plot of the cation $[Ni_3(depa)_4(PF_6)_2]^+$ from **4**·$3CH_2Cl_2$. Ellipsoids are drawn at the 30% probability level. Only one orientation of the disordered ethyl groups is shown; hydrogen atoms have been omitted for clarity.

but it may be observed here that in every case the Ni−N bonds for the center nickel atom are in the range 1.87−1.89 Å.

Nuclear Magnetic Resonance Spectra. Often, NMR spectra of paramagnetic compounds are difficult to detect or unobservable because of the short relaxation times exhibited by such compounds. Occasionally, a spectrum can be obtained, and sometimes interpretation is possible. We previously[6] reported the ^{1}H NMR spectrum of $Ni_3(dpa)_4Cl_2$ (**1**) in CD_2Cl_2 which showed four signals displaying large shifts and line-broadening at 48.79, 32.32, 15.69, and 9.08 ppm. This was consistent with a symmetrical molecular structure. The spectrum of $Ni_3(depa)_4Cl_2$ (**3**) recorded at room temperature in $CDCl_3$ is very similar except that the peak for **1** at 9.08 ppm is missing (see Table 3). This clearly identifies that peak as being due to the H(4) of the pyridyl

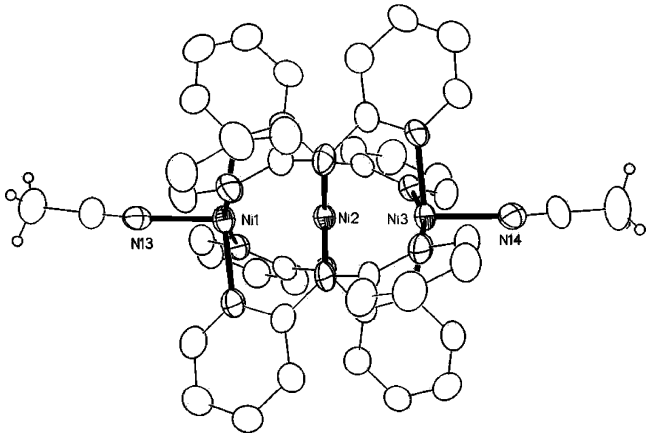

Figure 3. Thermal ellipsoid plot of the dication $[Ni_3(dpa)_4(NCMe)_2]^{2+}$ from **5**·$3.14CH_3CN$. Ellipsoids are drawn at the 50% probability level; pyridyl hydrogen atoms have been removed for clarity.

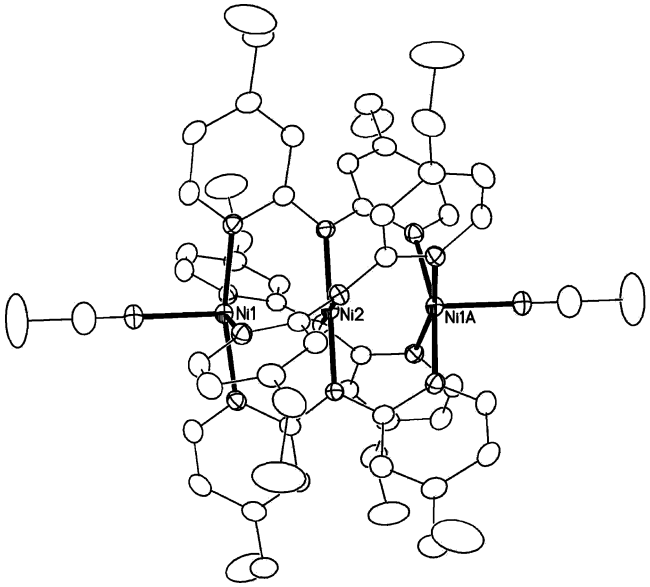

Figure 4. Thermal ellipsoid plot of **6** with ellipsoids drawn at the 40% probability level. Only the cation is shown; hydrogen atoms and solvent molecules have been omitted for clarity.

rings. The resonances for the ethyl groups are found as a peak at 1.301 ppm for the methyl groups and as two broad peaks at −0.430 and −0.816 ppm for the methylene protons. The reason for the splitting of the latter is not obvious.

The ^{1}H NMR spectrum for $[Ni_3(dpa)_4(CH_3CN)_2](PF_6)_2$ (**5**) is shown in Figure 5. While the chemical shifts are somewhat, but not greatly, different from those for **1**, the general similarity, especially for the line widths, is notable. There are also signals at 1.940 and 2.124 ppm, which we assign to CH_3CN and H_2O (present in the solvent), respectively. Thus, it appears that the coordinated CH_3CN molecules are exchanging with those in the solvent.

For $Ni_3(depa)_4(PF_6)_3$ (**4**) in CD_3CN, which has a completely different electronic structure from **3** and **5**, only three signals were observed: peaks at 2.002 and 1.585 ppm, in an approximate intensity ratio of 3:2, can be assigned to the CH_3 and CH_2 components of the ethyl groups; there is also a very broad signal (approximately 0.4 ppm width at half-height) centered at −3.44 ppm. This might be due to some

Table 2. Selected Internuclear Distances (Å) for Compounds **1**−**6**[a]

	1[b,c]	**2**[c]	**3**·0.5C_6H_{14}	**4**·3CH_2Cl_2	**5**·3.14CH_3CN	**6**·0.33H_2O
Ni−Ni	2.430[9]	2.284[1]	2.4325(3)	2.293[4]	2.374[2]	2.415(1)
Ni−N_1 outer	2.10[8]	1.927[5]	2.094[2]	1.930[6]	2.079[7]	2.071(3)
Ni−N_1 inner	1.89[6]	1.881[5]	1.893[1]	1.871[6]	1.882[8]	1.891(5)
Ni−Cl	2.33[4]		2.336(1)			
Ni···F		2.424, 2.429		2.458, 2.439		
Ni−$NCCH_3$					2.049[7]	2.037(7)
mean χ[d]	51.7	46.1	49.8	46.5	50.3	45.4

[a] Esds in parentheses when there is only one crystallographically distinct value. Esds in square brackets when several chemically equivalent but crystallographically distinct values have been averaged. [b] Averages from three independent structures discussed in ref 6. [c] Data from ref 7b. [d] χ is the average of the four torsion angles.

Table 3. Chemical Shifts (δ, ppm) from ^{1}H NMR Spectra

1 in CD_2Cl_2[a]	48.79	32.32	15.69	9.080
3 in $CDCl_3$	48.20	30.50	14.97	1.301 −0.430 −0.816
5 in CD_3CN	42.50	27.63	15.25	8.800

[a] From ref 6.

of the pyridyl protons, but the absence of other expected signals make an assignment difficult. Thus, the difference in the electronic structure of the oxidized species is also evident in the NMR spectrum. The numerical data for **1**, **3**, and **5** are presented in Table 3.

Electrochemistry. A solution of compound **3**, $Ni_3(depa)_4Cl_2$, in CH_2Cl_2 has a CV in the range 0−1.2 V that consists of a single reversible wave at an $E_{1/2}$ of 0.778 V, which may be compared with the behavior of **1**, $Ni_3(dpa)_4Cl_2$, in the same solvent, which has a wave at 0.908 V. Thus, the effect of the electron-donating ethyl groups is significant; they make the oxidation easier by 0.130 V. A similar effect has already been seen for the two Ni_5 species, $Ni_5(tpda)_4Cl_2$ and $Ni_5(etpda)_4Cl_2$.[1]

The effect of replacing the axial chloride ligands in $Ni_3(dpa)_4Cl_2$ (**1**) by acetonitrile molecules in $[Ni_3(dpa)_4(CH_3CN)_2]^{2+}$ is very striking. There is a shift of the $Ni_3(dpa)_4^{2+}/Ni_3(dpa)_4^{3+}$ couple to 1.205 V. While the direction is as expected, the magnitude of this shift, 0.297 V, is large enough to tempt one to think that other properties of the $Ni_3(dpa)_4^{2+}$ core might also be seriously altered, but, as shown later in this paper, they are not. In CH_2Cl_2 the oxidation of **1** is probably represented reasonably well by eq 4, while for the oxidation of **5** in CH_3CN, eq 5 is applicable. Removing an electron from a +2 ion to make the corresponding +3 ion as in eq 5 is bound to be more difficult than removing an electron from a neutral molecule to make the corresponding +1 ion in eq 4, even though the solvent for eq 5, CH_3CN, has a higher dielectric constant, namely, 38, than that for eq 4, CH_2Cl_2, where it is 9. In other words, the large shift is of mainly electrostatic origin and does not necessarily imply that the internal electronic structures (and hence bond lengths, bond angles, or magnetic properties) are very different. There is, however, a second redox wave for **5** centered at $E_{1/2} = 1.523$ V. This we assign to the process given in eq 6, which produces a $[Ni_3(dpa)_4]^{4+}$ ion. It should be noted that no $Ni_n^{(2n+2)+}$ species are known within the framework of four bridging ligands, and attempts are being made to isolate the Ni_3^{8+} unit from this system.

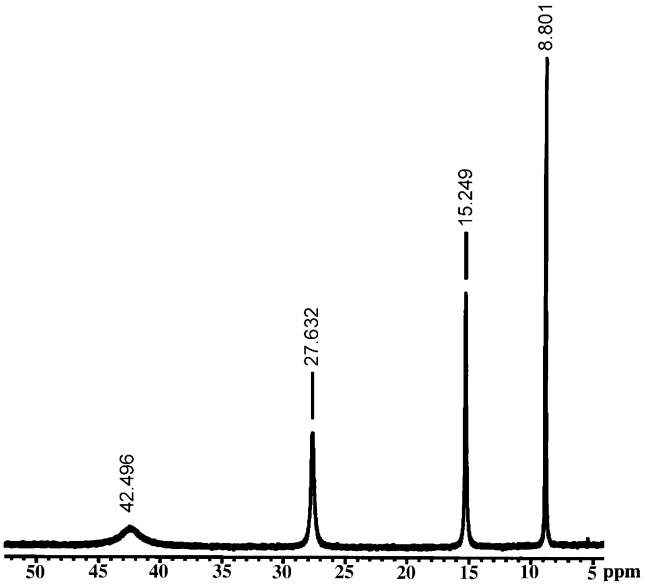

Figure 5. ^{1}H NMR spectrum of **5** taken at 300 MHz in CD_3CN at 23 °C.

This species is predicted to have a three-center four-electron σ bond along the trinickel chain.[7b]

$$Ni_3(dpa)_4Cl_2 = [Ni_3(dpa)_4Cl_2]^+ + e^- \quad (4)$$

$$[Ni_3(dpa)_4(NCMe)_2]^{2+} = [Ni_3(dpa)_4(NCMe)_2]^{3+} + e^- \quad (5)$$

$$[Ni_3(dpa)_4(NCMe)_2]^{3+} = [Ni_3(dpa)_4(NCMe)_2]^{4+} + e^- \quad (6)$$

Magnetic Susceptibility and EPR. Although the magnetic properties of **1** have been reported,[6,18] data were remeasured for a standardized comparison with the new Ni_3^{6+} compounds. These data are shown in Figure 6 and are consistent with two antiferromagnetically coupled high-spin Ni^{2+} ions in the terminal positions of the Ni_3 chains and a diamagnetic square planar Ni^{2+} species in the center. Therefore, eq 7 can be used to fit the data for **1**, **3**, **5**, and **6**:

$$\chi = \frac{6Ng^2\beta^2}{3kT}\frac{\exp(J/kT) + 5\exp(3J/kT)}{1 + 3\exp(J/kT) + 5\exp(3J/kT)} \quad (7)$$

This equation is based on the isotropic interaction between two $S = 1$ centers with the following Hamiltonian: $\mathscr{H} = -JS_1\cdot S_3 - g\beta S\cdot \boldsymbol{H}$. Here, N is Avogadro's number, g is the

(18) Note that there is a typographical error in ref 6. Since that work was done using the Hamiltonian $\mathscr{H} = -2JS_1\cdot S_3$, the value of J must therefore be half the value obtained here (using $\mathscr{H} = -JS_1\cdot S_3$). Thus, the expression "$2J = -108$ cm^{-1}" should read "$J = -108$ cm^{-1}."

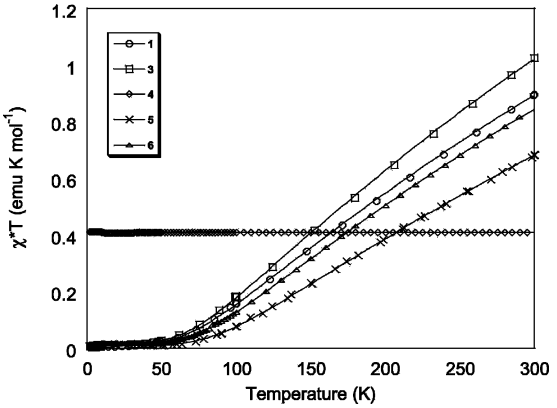

Figure 6. Magnetic susceptibility data for **1** and **3**−**6**. The solid lines represent the theoretical fits of the data (see text).

Table 4. Magnetic Susceptibility Results

	formula	J^a	g	R^b
1	$Ni_3(dpa)_4Cl_2$	−218.2(7)	2.067(5)	0.99998
3	$Ni_3(depa)_4Cl_2$	−217.5(7)	2.245(7)	0.99997
5	$[Ni_3(dpa)_4(CH_3CN)_2](PF_6)_2$	−267.6(5)	2.132(3)	0.99997
6	$[Ni_3(depa)_4(CH_3CN)_2](PF_6)_2$	−236.6(3)	2.197(2)	0.99998

[a] J (in cm^{-1}) is defined by the term $-JS_1 \cdot S_3$ for the spin−spin coupling. [b] R is the goodness of fit.

Landé factor, β is the Bohr magneton, k is Boltzmann's constant, J is the exchange parameter, and T is temperature. Also included were parameters accounting for paramagnetic $S = 1$ impurities (corresponding to less than 1% of the sample in every case) and TIP (in all cases $<300 \times 10^{-6}$ emu/mol).

The g values, shown in Table 4, are similar to each other and to those of typical paramagnetic nickel compounds.[19] Because the room-temperature χT values of **1**, **3**, **5**, and **6** are not the same, different values of J for each compound are to be expected. Indeed, the values of J for the complexes with axial acetonitrile ligands are more negative than those of the corresponding chloro complexes (see Table 4), indicative of stronger antiferromagnetic coupling in the former. Since the Ni···Ni distances in the acetonitrile complexes are shorter by 0.06 Å, it is possible that an important contribution to the exchange pathway between the terminal Ni^{2+} ions is through direct Ni···Ni interaction. This has also been seen in the $Cu_3(dpa)_4X_2$ system, where the Cu···Cu distances of 2.47 and 2.40 Å for $Cu_3(dpa)_4Cl_2$ and $Cu_3(dpa)_4(BF_4)_2$, respectively, led to stronger antiferromagnetic coupling in the latter.[20]

In contrast, there is no temperature dependence of χT for the oxidized compound **4** (see Figure 6). The χT value of 0.406 emu·K/mol corresponds to one unpaired electron with $g = 2.08$.

The EPR spectrum of **4** shows an axial signal with $g_\perp = 2.165$ and $g_\parallel = 2.117$. The signal for $g_\parallel$ was split into a triplet with $A_\parallel = 150$ G. This is similar to that of **2**.[7b] Both are consistent with the presence of one unpaired electron and show axial symmetry with $g_\parallel > g_\perp$ and hyperfine splitting. This is likely due to the interaction of the unpaired electron with the two $I = {}^1/_2$ ^{19}F nuclei in the axial positions of the molecules. It is interesting that this coupling is observed, despite the long Ni···F distances of >2.4 Å in the solid state. Furthermore, the existence of this splitting supports the electron delocalization along the Ni_3^{7+} unit as the unpaired electron sees equally well each of the terminal PF_6 anions.

4. Additional Remarks

Comparison of 1 and 3. The introduction of the two 4-ethyl substituents, that is, changing from $Ni_3(dpa)_4Cl_2$ to $Ni_3(depa)_4Cl_2$, has essentially no structural effect. Both molecules have essentially symmetrical structures with D_4 symmetry in the $Ni_3N_{12}Cl_2$ cores. To within 0.01 Å the corresponding bond lengths are the same, including the Ni−N distances despite ca. 0.8 difference in the pK values of the pyridyl and 4-ethylpyridyl groups.[21] In five separate crystal structures of **1** the overall torsion angle ranged from 49.6° to 53.2°, while in **3** the torsion angle is in the range 49.1−51.2°.

Electrochemically, there is a significant and helpful difference. For both **1** and **3** there is a reversible, one-electron oxidation, but for **3** oxidation is more than 100 mV easier ($E_{1/2} = +0.778$ V vs Ag/AgCl in CH_2Cl_2) than in **1** ($E_{1/2} = 0.908$ V vs Ag/AgCl in CH_2Cl_2), in keeping with the greater basicity of the ethyl-substituted ligand.

Oxidations To Produce 2 and 4. Reaction of purple **1** or **3** with 3 equiv of $AgPF_6$ in CH_2Cl_2 gives the corresponding blue compounds $Ni_3(dpa)_4(PF_6)_3$[7] or $Ni_3(depa)_4(PF_6)_3$ in isolated yields of better than 75%. Structurally **2** and **4** are very similar. In both compounds there is a highly significant decrease in the Ni−Ni separations upon oxidation. For **2** there are two crystallographically independent Ni−Ni separations of average value 2.284[1] Å which are ca. 0.15 Å shorter than those of **1**.[7] For **4**, there are also two crystallographically independent but chemically insignificant separations of 2.296(1) and 2.289(1) Å. These are ca. 0.14 Å shorter than those in the precursor **3**. In both precursors there are Ni−Cl distances of ∼2.33 Å, but in **2** and **4** the axially situated PF_6 anions are relatively far away (Ni···F separations of over 2.4 Å). There is also a significant shortening of the Ni−N distances for **2** and **4** as compared to those in the precursors, clearly attributable to the increase in overall positive charge which would be expected to increase attraction for the nitrogen donor atoms. The greater effect is observed on the outer Ni−N distances. For **2**, the central Ni−N distances are 1.881[5] Å and the outer ones are 1.927-[5] Å.[7] These are significantly shorter than the corresponding distances (1.89 and ∼2.10 Å, respectively) in **1**.[7b] A similar situation is found in the **3**/**4** couple where the outer Ni−N distances are in the ranges 2.086(2)−2.101(2) and 1.918-(6)−1.940(6) Å.

It is clear that the large shortening in Ni−Ni separation upon oxidation would not be expected for nonbonded metal

(19) Drago, R. S. *Physical Methods in Chemistry*; W. B. Saunders Company: Philadelphia, 1977; p 486.
(20) Berry, J. F.; Cotton, F. A.; Lei, P.; Murillo, C. A. *Inorg. Chem.* **2003**, *42*, 377.
(21) Martell, A. E.; Smith, R. M. *Critical Stability Constants*; Plenum Press: New York, 1982.

atoms in **1** and **3** if they remained nonbonded. An increase in the total chain charge from Ni_3^{6+} to Ni_3^{7+} would be expected to increase repulsion between the positively charged nickel ions. Such an increase has been shown by oxidizing $Cu_3(dpa)_4Cl_2$ to $Cu_3(dpa)_4Cl_2^+$ where the Cu···Cu separation increases by 0.04 Å from 2.47 to 2.51 Å.[7b] Neither one of these compounds has metal−metal bonds. Therefore, the shortening by ca. 0.15 Å of the metal−metal distance in the trinickel compounds must be attributed to metal−metal bond formation. This is consistent with transformation to a delocalized system that is likely to be a conductor. We believe that these molecules could therefore serve as on−off switches, which could be controlled by an applied oxidation potential. They could also be expected to serve as physical switches as the length of the Ni_3 unit decreases by 0.30 Å upon oxidation.

An especially interesting observation is the great increase in thermal stability of the ethyl-substituted **4** versus that of the unsubstituted **2**. The latter is stable as a solid and in solution but only at low temperatures. However, **4** appears to be stable indefinitely at room temperature. This improved stability is presumably associated with the significant decrease in the oxidation potential of the ethyl-substituted precursor, as mentioned above.

In parallel work[1] we have shown that this effect is observable in longer EMACs and the corresponding five-metal chains are more readily oxidized than the unsubstituted ones and thermally stable also. Another important advantage of the ethyl-substituted compounds is a significant increase in solubility relative to the corresponding unsubstituted compounds. This factor should be of great value as the length of the EMAC increases.

Comparisons of 1 and 5 and of 3 and 6. The replacement of axial Cl^- ligands by axial CH_3CN ligands has several major effects on the Ni_3N_{12} core. There is considerable shortening of the Ni···Ni distances, from values in the range of 2.417(1)−2.443[1] Å in **1** to 2.374[2] Å in **5**. At the same time, the corresponding (i.e., inner and outer) equatorial Ni−N distance scarcely change and the difference between them remains 0.20 Å. Even though the Ni···Ni distances shorten by about 0.06 Å, it would be expected that, as in **1**, there would be no Ni−Ni bonding in **5**, and this is borne out by the magnetic data. Both **1** and **5** are to be viewed as having inner $S = 0$ Ni(II) atoms and outer Ni(II) atoms with $S = 1$, with magnetic spin coupling between the two outer magnetic moments. However, there is a significant increase, from −216 to −268 cm^{-1} in the magnitude of the coupling constant (in the term $-JS_1 \cdot S_3$), on going from **1** to **5**. This probably indicates that at least some (perhaps all) of the coupling is transmitted through the central nickel atom since it accords well with the decrease in Ni···Ni distances whereas the entire indirect path from Ni(1) to Ni(3) via the Ni−N−C−N−C−N−Ni chains does not appear to be significantly changed as has been demonstrated for Cu_3 compounds.[21] Similar results are found in the cases of **3** and **6**, although the difference in J is not as pronounced.

5. Concluding Remarks

The effect of introducing the ethyl substituents to **1**, **2**, and **5** so as to obtain **3**, **4**, and **6** is 2-fold. First, as expected and intended, it increases the solubilities. We are thus reporting the first examples of what will be an extensive, planned program of making EMACs of many lengths and with many metals that will have better solubilities than do those of dpa and its longer homologues, loosely called polypyridyl amides.

The second important effect is how the introduction of alkyl substituents changes the redox chemistry. The electron-donating influence of the ethyl groups makes oxidized species significantly easier to obtain and improves their stability. We have an excellent illustration of this not only in comparing the redox potentials of **1** and **3** but in a very practical sense by the greater thermal stability of **4** compared to **2**. There was an expectation of such an effect from the fact that 4-ethylpyridine is considerably more basic than pyridine by about 0.8 pK units. It has been a pleasant surprise to see how well this has translated into the measured and observed properties of the trinickel EMACs.

Acknowledgment. This work was supported through a Nanoscale Science and Engineering/NIRT Grant (DMR-0103455) and the Telecommunications and Information Task Force at Texas A&M University. J.F.B. thanks the National Science Foundation for support in the form of a predoctoral fellowship. We also thank Dr. A. Murali and Mr. C. Fewox for assistance in the EPR measurements and Peng Lei for assistance in obtaining NMR spectra.

Supporting Information Available: X-ray crystallographic data in CIF format for **3**·0.5hexane, **4**·$3CH_2Cl_2$, **5**·$3.14CH_3CN$, and **6**·$0.33H_2O$ and EPR spectrum for **4** as a PDF file. This material is available free of charge via the Internet at http://pubs.acs.org.

IC0341486